SITE RESPONSE MODELING IN LIQUEFIABLE SOIL DEPOSITS

Steven L. Kramer
University of Washington
Seattle, WA 98105
USA

Aaron J. Hartvigsen
Geoengineers
Bellingham, WA
USA

Samuel S. Sideras
University of Washington
Seattle, WA 98105
USA

Pelin T. Ozener
Yildiz Technical University
Istanbul
Turkey

ABSTRACT

Soil liquefaction is a phenomenon most commonly associated with ground failure, but which also can have a significant effect on earthquake ground motions. Accurate prediction of site response for profiles containing potentially liquefiable soil is important for evaluation of existing structure vulnerability and for design of new structures. The state of the art in this area has advanced significantly in recent years as the mechanics of cyclically loaded soils approaching and following the initiation of liquefaction has become better understood. The state of practice, however, lags somewhat behind due to the unavailability of computational tools that properly capture liquefiable soil behavior. As performance-based concepts work their way into geotechnical earthquake engineering practice, the need for more accurate modeling of liquefiable soil profiles will only increase.

This paper reviews recent developments in the modeling of liquefiable soils with a particular focus on the phase transformation behavior that affects cyclic and permanent strain amplitudes. It then discusses common characteristics of ground motion recordings affected by liquefaction. The role of vertical arrays in the validation of site response models is described. Finally, the results of an investigation of the effects of liquefaction on ground motions, from the standpoints of time histories and response spectra computed using both total and effective stress analyses are presented.

INTRODUCTION

Soil liquefaction has caused extensive damage to structures and constructed facilities in past earthquakes. While liquefaction-induced ground failure, such as that caused by lateral spreading and post-earthquake settlement, gain a great deal of attention following earthquakes, the occurrence of liquefaction also affects ground motions beneath structures and their foundations. The reliable and economical seismic design of structures requires that ground motions be reliably predicted. When these structures are underlain by liquefaction-susceptible soils, prediction of site response – before, during, and after initiation of liquefaction – is required.

This paper describes the behavior of liquefiable soils, some of the challenges involved in predicting the response of soil profiles containing liquefiable soils, and the effects of liquefaction on ground surface motions. The paper focuses on those aspects of constitutive behavior that are unique to liquefiable soils, their effects on site response, and the challenges they present in site response modeling in liquefiable soils.

BEHAVIOR OF LIQUEFIABLE SOILS

Not all soils are susceptible to liquefaction. In the field, liquefaction has been observed in loose, saturated, clean and silty sands and in gravelly soils confined by less permeable soil or rock layers. Liquefaction results from the buildup of excess porewater pressure, hence it occurs most readily in highly contractive soils such as loose, uniform sands and non-plastic silts. Soils of high plasticity or soils containing significant amounts of plastic fines are generally considered non-susceptible to liquefaction.

1

The behavior of liquefaction-susceptible soils subjected to cyclic loading has been studied for nearly 50 years. Laboratory studies applying constant-amplitude, periodic (generally harmonic) shear stresses have been used by numerous researchers to investigate the rate of pore pressure generation, and its dependence on factors such as soil density, initial effective confining pressure, and shear stress amplitude. Early studies showed that rates of pore pressure generation increased, all other things being equal, with decreasing density and increasing (normalized) shear stress amplitude; the results of laboratory tests are typically reported in terms of curves relating number of cycles to liquefaction to normalized shear stress amplitude, e.g., cyclic stress ratio, CSR (Fig. 1) and curves showing the rate of pore pressure generation up to the point of initial liquefaction (Fig. 2). Later experimental investigations showed that laboratory liquefaction resistance was also influenced by a number of other factors (e.g., soil fabric, prior strain history, etc.) that existed in the field but could not be reliably replicated in the laboratory. As a result, the evaluation of liquefaction resistance moved from a laboratory basis to a basis rooted in the interpretation of field case histories.
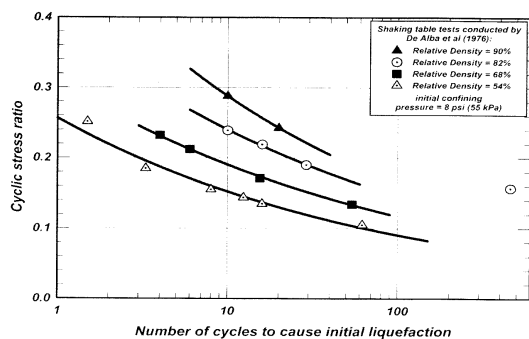

Fig. 1. Liquefaction resistance curves from laboratory tests (after Idriss and Boulanger, 2008).
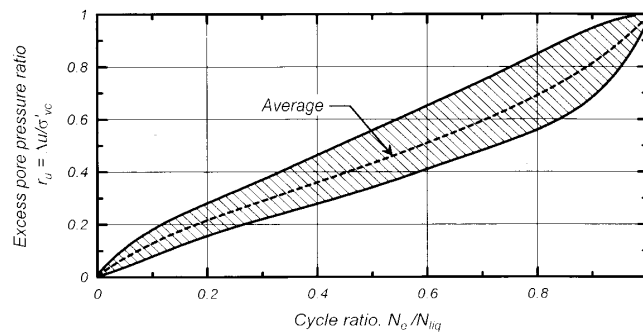
Fig. 2. Rate of pore pressure generation in liquefiable soils (Idriss and Boulanger, 2008).

Laboratory tests still provide very useful insight into the behavior of liquefiable soils, and are of great value in developing constitutive models that describe their behavior. In the early stages of a typical cyclic loading test, the generation of excess pore pressure causes the stiffness of the soil to decrease (Fig. 3a) and the effective stress path to move to the left (Fig. 3b). The pore pressure initially increases quickly (as in Fig. 2), but its rate of generation then slows until the stress path begins to cross the phase transformation line (PTL). At the PTL, the soil changes from contractive to dilative behavior so that the effective stress increases under increasing loading above the PTL. Upon stress reversal above the PTL, the soil becomes more contractive and the rate of pore pressure generation increases from cycle to cycle until the effective stress eventually reaches zero. At this point, the soil exhibits a very low shear modulus but, unless it is extremely loose, dilates upon increasing shear stress and gains stiffness until the shear stress is reduced. Repeated constant amplitude loading cycles results in a stabilized effective stress path in which the soil moves from contractive to dilative states twice within each loading cycle. The stress-strain behavior follows the effective stress path behavior, with the shear modulus depending on the strain level but also the level of effective stress, giving rise to the familiar "banana-shaped" hysteresis loops observed in the laboratory. Laboratory tests show that the shear strain amplitude continues to increase even when the effective stress path has stabilized, indicating that some additional mechanism is affecting the stiffness of the soil under these conditions. Most models attribute this additional component of softening to alteration of the soil fabric that occurs when the soil is at a state of nearly zero effective stress.

Under conditions of no static shear stress (i.e., similar to level-ground) conditions, the shear strain increases roughly equally in the positive and negative conditions. When some non-zero initial shear stress exists, as in the case of an element of soil under sloping ground conditions, shear strains accumulate preferentially in the downslope direction. The dilative tendencies of the soil when subjected to shear stresses above the PTL, however, are extremely important in limiting the downslope displacements that can develop after generation of high pore pressures.
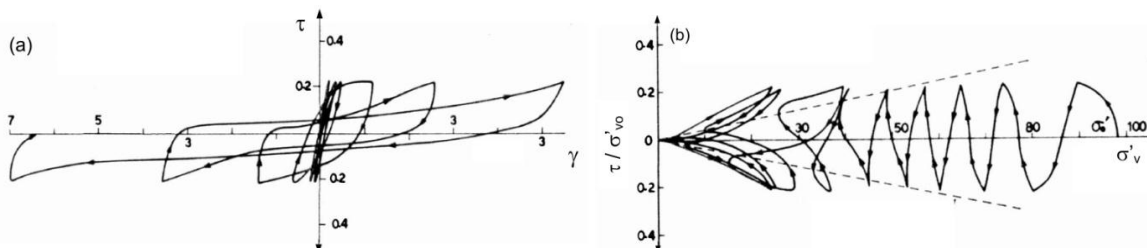

Fig. 3. Behavior of liquefiable soils subjected to constant-amplitude cyclic loading: (a) stress-strain, and (b) stress path behavior (after Ishihara, 1985).

2

MODELING OF LIQUEFIABLE SOILS

A constitutive model for liquefiable soils must model the nonlinear, inelastic behavior of the soil skeleton in shear as would be required for a total stress analysis of the soil. However, the behavior of liquefiable soils is dominated by pore pressure generation so the constitutive model must also model the volumetric behavior under cyclic loading conditions. The former of these requirements is generally relatively straightforward – many total stress nonlinear models are available and generally capable of representing the total stress behavior of sandy soils for nonlinear site response analysis. Perhaps the most difficult issue in modeling total stress behavior is the simultaneous representation of stiffness degradation and energy dissipation. Many total stress models rely on a backbone curve and unloading-reloading "rules" such as the Masing rules (Masing, 1926) or Cundall-Pyke hypothesis (Pyke, 1979). Such rules relate the shape of an unloading curve to the backbone curve; as a result, the shape of a hysteresis loop, which controls the damping ratio, is uniquely related to the rate of stiffness degradation. In most cases, models calibrated to match a given rate of stiffness degradation (e.g., a particular modulus reduction curve) will overpredict the expected damping (i.e., the corresponding damping curve). Different approaches to the solution of this problem have been proposed (Muravskii, 2004; Phillips and Hashash, 2009), but have not yet been implemented in widely used nonlinear site response codes.

Early nonlinear models (e.g., Martin et al., 1975) sought to predict the cycle-by-cycle generation of excess porewater pressure up to the point of liquefaction and paid relatively little attention to the behavior of the soil after the initiation of liquefaction (other than to note that the soil became very soft and weak). The rate of pore pressure generation up to the point of initiation was characterized (Fig. 2) and used as the basis for the cycle-by-cycle methods; these models did not attempt to replicate the pore pressure (hence, normal stress and stiffness) changes that would occur *within* individual loading cycles. Such models account for the generation of porewater pressure by softening and weakening the soil as a function of pore pressure ratio. Since the pore pressure increases monotonically, the stiffness decreases monotonically and can reach very low values at high pore pressure ratios. When such high levels of pore pressure develop, the soil can become so weak that its ability to transmit shear stress is limited – beyond that point, the liquefied layers act to isolate the overlying soil from significant shaking.

In recent years, more advanced constitutive models (e.g., Iai et al., 1990; Manzari and Dafalias, 1997; Yang et al., 2003) have shown the ability to predict pore pressure fluctuations observed both within and between individual cycles prior to, during, and after the initiation of liquefaction in constant-amplitude, harmonic loading laboratory tests. These models, when implemented into nonlinear site response codes, offer the potential to represent the known behavior of soils more accurately than the simpler, cycle-by-cycle models. They can also reproduce important features of liquefiable soil profile response that have only been recognized relatively recently.

CHARACTERISTICS OF GROUND MOTIONS AFFECTED BY LIQUEFACTION

The occurrence of liquefaction can affect ground surface motions in a number of ways. While the behavior of a specific soil profile will depend on the details of its interaction with a particular motion, some general aspects of liquefiable soil profile behavior can be observed.

Effects of Pore Pressure Generation.

As excess pore pressure builds, effective stresses decrease and the shear modulus of the soil, which tends to vary with approximately the square root of effective stress, also decreases. There is, therefore, a reduction in profile stiffness that tends to decrease the profile's tendency to transmit high frequency waves and increase its tendency to transmit low frequency waves. This change in transmission characteristics generally occurs relatively gradually in the early stages of shaking when pore pressure ratios are low and may or may not have a noticeable effect on ground surface motions depending on the evolving frequency content of the excitation.

As excess pore pressures reach higher values, however, the rate of softening increases and the rate of pore pressure generation increases as the effective stress paths of critically stressed elements within the profile begin to cross the PTL. The combination of these two effects form a sort of positive feedback loop that can cause profile softening to occur very quickly near the initiation of liquefaction. For many profiles, particularly those that include very loose soils, the result is a rapid change in the frequency content of the surface motion. As illustrated in a recording from the basement of a Kawagishi-cho apartment building in the 1964 Niigata earthquake (Fig. 4), the high frequencies that dominate the first seven seconds of the motion are of reduced amplitude riding on a low frequency carrier from about 7–12 sec, and then virtually disappear after 12 sec. The motion at $t > 12$ sec has a period of 5–6 sec. Time-frequency plots can show the evolving frequency content of the Kawagishi-cho motion. Figure 5 shows short-term Fourier transform (STFT), wavelet, and Stockwell (S-transform) plots for the Kawagishi-cho NS motion. All three plots show a dramatic reduction in amplitude and predominant frequency after approximately 11–12 sec.
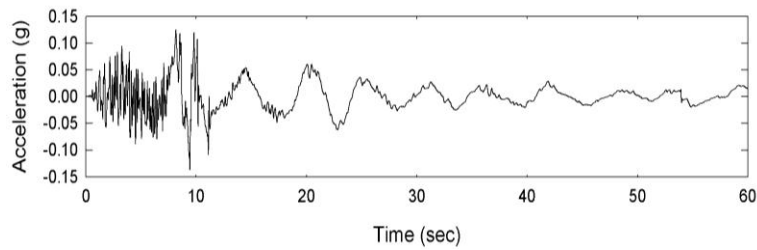
Fig. 4.Time history of NS component of ground motion measured in basement of Kawagishi-cho apartment building in 1964 Niigata earthquake.
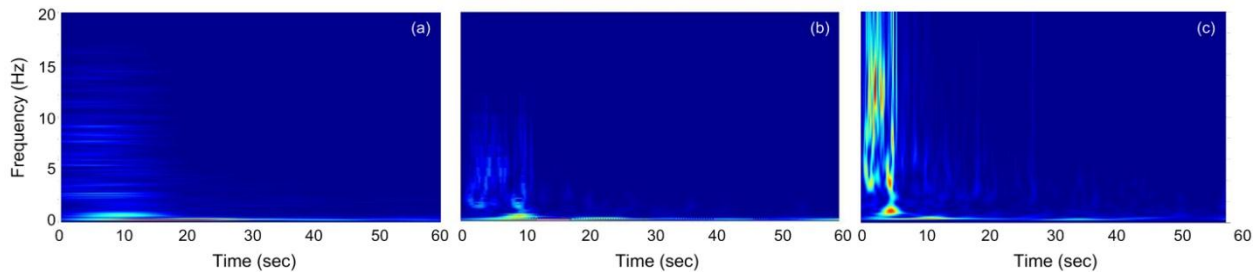

Fig. 5. Variation of acceleration amplitude with time and frequency for ground motion measured in basement of Kawagishi-cho apartment building in 1964 Niigata earthquake: (a) short-time Fourier transform, (b) wavelet transform, and (c) Stockwell transform.

Effects of Phase Transformation Behavior

The soil profile at Kawagishi-cho (Ishihara, 1985) contains several meters of extremely loose sand whose dilative characteristics are limited by its very low residual strength. As a result, the soil profile becomes very soft upon the triggering of liquefaction, and it remains very soft over the duration of shaking. In denser sand, dilation with consequent stiffening will occur as shear stresses increase. As a stress pulse involving dilation develops at the base of a dilating soil layer, the initial portion of the stress pulse propagates slowly because the effective stress, and hence the stiffness, is very low. As the amplitude of the shear stress increases, dilation causes the effective stress, and stiffness, to increase so that the later portion of the stress pulse travels faster than the early portion. This causes the later portion of the pulse to "catch up" to the early portion and results in a temporal focusing of the energy in the pulse. The resulting phenomenon, referred to as "de-liquefaction shock waves" by Kutter and Wilson (1999), can result in sharp, high-frequency spikes of acceleration superimposed upon the long-period response of the softened soil.

Vertical arrays have been installed in potentially liquefiable soil profiles at a number of locations around the world. To date, relatively few have been subjected to earthquake shaking sufficiently strong to trigger liquefaction. The most well-known and widely studied of these arrays is the previously described Wildlife Liquefaction Array (WLA). The Wildlife site consisted of 2.5 m of lean clay/silt underlain by 1 m of sandy silt above 3.3 m of loose, silty sand. The silty sand was, in turn, underlain by highly plastic clay within which a downhole instrument was placed at a depth of 7.5 m. A series of piezometers was installed in the silty sand. The Wildlife array was subjected to strong shaking in 1987 from the Elmore Ranch and Superstition Hills earthquakes. The Elmore Ranch earthquake of November 23, 1987 was a M6.2 event epicentered 23 km west of the WLA and did not produce surficial evidence of liquefaction. The Superstition Hills earthquake, a M6.6 event that occurred about 11 hrs later, produced sand boils, ground fissures, and permanent lateral displacements at the site. The WLA piezometers recorded pore pressure signals that appeared lower than expected, and that have been the subject of some controversy over the years (Earth Technology Corporation, 1991;Hushmand *et al.*, 1991, 1992; Youd and Holzer, 1994; Scott and Hushmand, 1995).

Figure 7 shows the NS component of the Wildlife record from the 1987 Superstition Hills earthquake. Visually, the high-frequency portion of the motion appears to diminish significantly at about 18 sec; however, there are a series of isolated, high-frequency pulses of acceleration after that point, most notably at 20, 21, 22, 31, 35, 37, and 54 sec. Zeghal and Elgamal (1994) correlated these pulses to temporary drops in measured pore pressures and proposed that they were cause by dilation-induced stiffening. Time-frequency plots (Fig. 8) show these pulses, with varying degrees of resolution, as light-colored vertical stripes; these plots also suggest that the amplitude of high-frequency components decreased markedly after about 14 sec of shaking. In many cases, these pulses have amplitudes smaller than those of the pulses that occur prior to liquefaction, but in some cases the PGA of the entire motion is associated with dilation pulses.
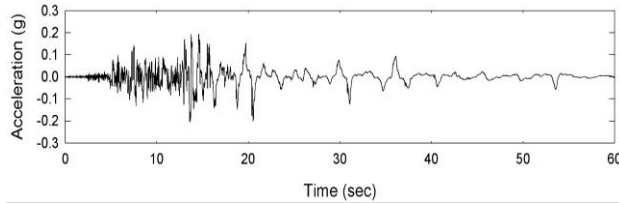
Fig. 7. Time history of NS component of Wildlife ground surface motion in 1987 Superstition Hills earthquake.
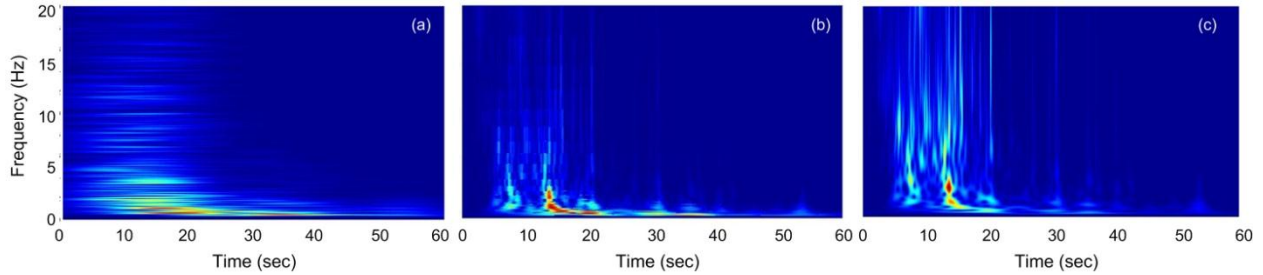

Fig. 8. Variation of acceleration amplitude with time and frequency NS component of Wildlife ground surface motion in 1987 Superstition Hills earthquake: (a) short-time Fourier transform, (b) wavelet transform, and (c) Stockwell transform.

Time-Dependent Amplification Behavior

The degree to which changes in the frequency content reflect the behavior of a liquefiable soil within the deposit depends on the nature of the input motion. In many cases, the transition from body-wave to surface-wave-dominated portions of a bedrock motion leads to a shift toward lower frequencies in the ground surface motion. Some of the reduction in frequencies of the surface motion, therefore, can result from changes in the frequency content of the underlying rock motion. Ideally, these effects could be minimized by comparing the motions immediately above and below the liquefiable layer, e.g. by computing spectral ratios of such motions. Unfortunately, very few sites have been instrumented in such a way as to allow spectral ratios to be computed. The Wildlife site, which liquefied in the 1987 Superstition Hills earthquake, had accelerometers at the ground surface and in stiff soil just below a 3.3-m-thick layer of loose, saturated silty sand. Cross-correlation of the early portion of the surface and downhole motions was maximized at a time lag of 0.082 sec, which implies an average shear wave velocity of about 93 m/sec in the upper 7.5 of the profile. This value, which is generally consistent with V_s measurements in the area, implies a quarter-wavelength frequency of approximately 3 Hz for the upper 7.5 m of the Wildlife site. Time-dependent spectral ratios can be obtained by taking the ratios of spectral amplitudes from STFT, wavelet, or Stockwell-transform spectra. Because the amplitudes of all three spectra vary irregularly with frequency at a given point in time, spectral ratios are generally easier to interpret when computed with spectra that are first smoothed. Figure 9 shows surface and downhole accelerograms along with ratios of Stockwell-transform spectra for the Wildlife NS ground motion.

Spectral ratio plots provide a graphical indication of which frequencies are more and less strongly amplified over the duration of a ground motion. In Fig. 9, the characteristic site frequency of approximately 3 Hz is indicated by the pervasively high ratios in that frequency range from about 3 – 13 sec. After about 13 sec, however, the ability of the Wildlife profile to amplify frequencies in that range drops sharply. At higher frequencies, the ratio is quite low except for brief periods of time in which dilation-induced stiffening allows higher-frequency pulses to reach the ground surface. The variation of average spectral ratio in a band from f_o to $2f_o$ (3-6 Hz) with time is shown in Fig. 10; preliminary examination of a number of ground motion recordings affected by liquefaction suggest that a rapid decrease in spectral ratio at and above the initial characteristic site frequency is indicative of the initiation of liquefaction. On this basis, liquefaction at the Wildlife site is judged to have been triggered at $t = 12.5 – 13.0$ sec.
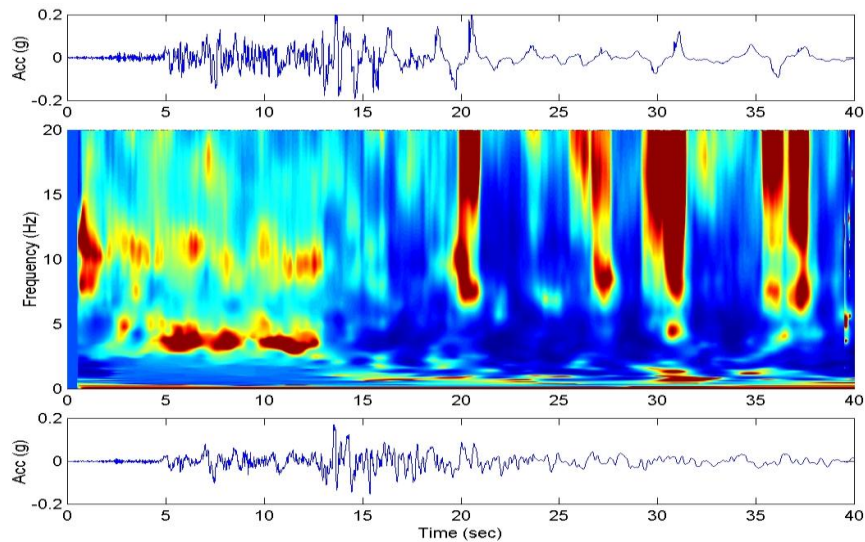
Fig. 9.Downhole and surface NS time histories with time-frequency plot of Stockwell spectral ratio. Warmer colors represent higher ratios – the deepest blue represents a ratio of zero and the deepest red represents ratios of 5 or greater.
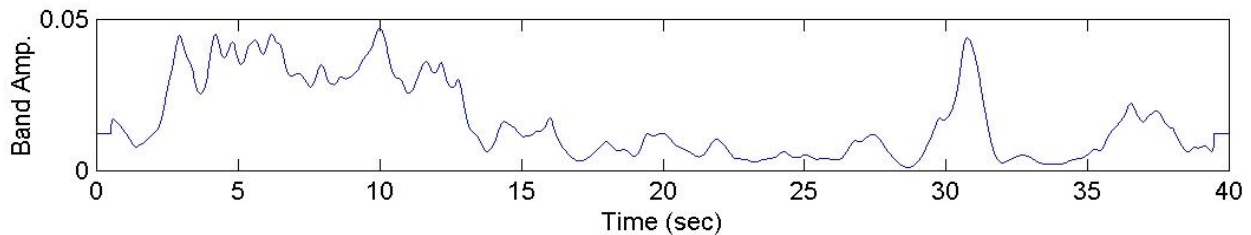

Fig. 10. Variation of average spectral ratio in 3 Hz – 6 Hz band with time. Rapid drop from 12.5-13.0 sec taken to indicate initiation of liquefaction.

In most cases, recordings of downhole motions are not available. For many vertical arrays, the downhole instrument is so far below the base of the liquefiable layer than the spectral ratio is strongly influenced by the soil between the liquefiable layer and the downhole instrument. To attempt to detect variations in the ability of a soil profile to transmit higher frequency waves, the use of H/V spectral ratios was explored. H/V ratios have been used (e.g., Nakamura, 1989) to identify characteristic site frequencies based on active or ambient vibrations.

To investigate the potential for such an approach to indicate the initiation of liquefaction, spectral ratios were computed using surface horizontal and vertical recordings. Figure 11 shows Stockwell spectral ratios for the Wildlife NS record – while the colormap induced pulses, the amplitude in the 3-6 Hz band (Fig. 12a) does not show a sharp drop in that area. Interestingly, the band amplitude for the EW component (Fig. 12b) does show a relatively sharp drop in the 12-15 second range.

Identification of the timing of liquefaction has important consequences for evaluation of liquefaction potential and the effects of liquefaction. Mayfield (2007) estimated the time of initiation from six records and used that information to determine the value of an evolutionary intensity measure, CAV5, at those times. Similar calculations can be performed with intensity measures such as Arias intensity and even cyclic stress ratio to identify data points that are on (rather than above or below) a liquefaction resistance curve, as done by Mayfield (2007).
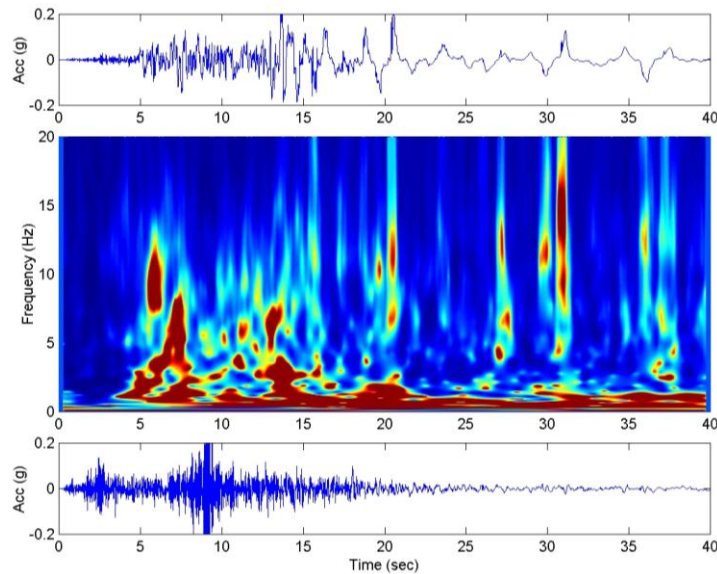
Fig. 11.Surface Wildlife NS (upper) and vertical (lower) time histories with time-frequency plot of Stockwell spectral ratio. Warmer colors represent higher ratios – the deepest blue represents a ratio of zero and the deepest red represents ratios of 5 or greater.

(a)   (b)
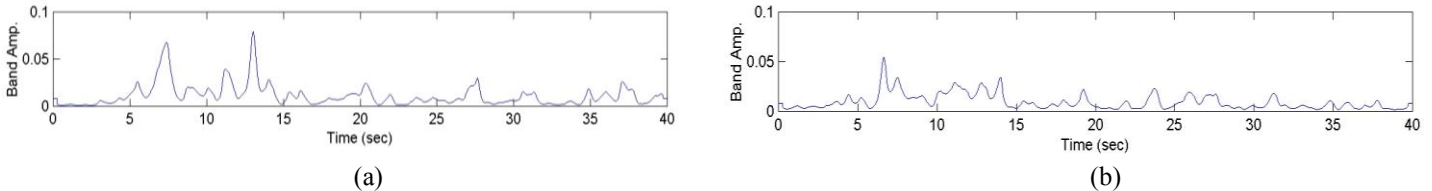
Fig. 12. Average 3-6 Hz band amplitudes for Stockwell spectral ratio of surface horizontal to surface vertical motions: (a) Superstition Hills NS, and (b) Superstition Hills EW.

ANALYSIS OF VERTICAL ARRAYS

A number of investigators have analyzed the response of the WLA to the Superstition Hills earthquake. These analyses have used equivalent linear techniques (e.g. Youd and Carter, 2005) and a variety of nonlinear techniques ranging from models with relatively simple, monotonically-increasing pore pressure models (Martin et al., 1975; Dobry et al., 1985) to sophisticated constitutive models (Iai et al., 1990; Manzari and Dafalias, 1997; Yang et al., 2003), and virtually all have been performed using one-dimensional analyses. The goal of such modeling has usually been the validation of a particular numerical code, with validation being evaluated by the degree to which the calculated ground surface motion matched the recorded motion.

The degrees to which the analyses have successfully predicted the recorded ground surface motions have varied with the type of analysis performed. Youd and Carter (2005) analyzed the WLA profile using the downhole records from both the Elmore Ranch and Superstition Hills earthquakes using the equivalent linear program, ProShake. Youd and Carter obtained good agreement between the recorded and predicted time histories and response spectra for the entire Elmore Ranch and for the first 13 sec of the Superstition Hills record. However, the predicted motions were very different than the recorded motions after 13 sec, which Youd and Carter took as evidence that significant softening of the soil profile began at about 13 sec. Bonilla et al. (2005) used a multishear mechanism model developed by Iai et al. (1990) in a one-dimensional finite difference code and were able to compute surface motions that agreed well with the recorded motions both before and after the initiation of liquefaction; the good agreement came with pore pressures generated at a much faster rate than was recorded in the field.

Challenges

There are a number of challenges in the validation of site response analyses using vertical array data, and these challenges must be kept in mind when evaluating the results of such studies. The following sections briefly describe some of the most significant of these challenges.

7

Site Characterization. Different site response models require different input parameters, primarily due to the different stress-strain or constitutive models used to represent soil behavior. While equivalent linear models use familiar modulus reduction and damping curves, nonlinear models generally require parameters that describe yield surfaces, hardening laws, and flow rules – some of these parameters have physical meaning and others may not, or may require non-routine testing to determine. Some soil profile characteristics, for example permeability, may be very difficult to characterize at a scale that may be significant with respect to pore pressure and site response behavior.

Dimensionality. Vertical arrays in liquefiable soils are nearly always analyzed using one-dimensional procedures. The one-dimensional approach is commonly used because it captures the main waveforms that produce horizontal site response. One-dimensional analyses cannot capture surface wave and basin effects, and usually do not account for inclined waves, all of which can have significant effects on the response of some sites. One-dimensional analyses also neglect lateral heterogeneities that can suppress high frequency response such as that associated with dilation pulses.

Directionality. Strong motion recordings include three components of ground motion, but nearly all site response analysis codes consider only a single component of motion at a time. While vertical motions are not thought to significantly affect liquefaction, the generation of excess pore pressure in liquefiable soils has been shown to be affected by out-of-plane horizontal motions (Pyke, 1973; Boulanger and Seed, 1995). Most validation exercises using vertical array data perform independent analyses for the two orthogonal horizontal components and generally produce different rates of pore pressure generation for the two cases.

Repeatability. Nearly all nonlinear models can be manipulated to optimize their predictions for a single ground motion recording. In some cases, applying the optimized model to a different recording at the same site produces a poor prediction of the recorded motion. A proper model validation should include predictions of different motions, preferably at the same site, using a single set of model parameters. The ability to accurately predict response to both weak and strong levels of shaking is the hallmark of a capable model.

Crust Behavior. Most liquefiable soil profiles have a surficial layer, or crust, of non-liquefied soil. The crust may be composed of dry or partially saturated soil above the water table or of a soil type that is not susceptible to liquefaction. In the field, the softening that results from high pore pressures causes large deformation of the crust, often accompanied by significant distortion and cracking. These mechanisms, which affect the gross characteristics of the crust, are not explicitly modeled in typical site response analyses; in such analyses, the crust remains intact with significant stiffness. Since the recording instrument is on the crust, its motion may be influenced by phenomena that site response analyses are unable to represent. In some cases, the soil immediately beneath a crust of thickness, H, becomes so soft that the crust is effectively decoupled from the soil profile and responds with a "free-free" standing wave at a period $2H/V_s$, that adds a lightly damped, high-frequency harmonic motion to the computed surface motion. Degradation of crustal stiffness (with increase in crustal damping) following the initiation of liquefaction can alleviate this problem, but no data upon which to base such degradation is available.

Soil-Structure Interaction. Strong motion instruments are generally attached to a concrete foundation embedded to some depth within the near-surface soil and covered by some form of instrument shelter. Crouse and Hushmand (1989) investigated soil-structure interaction effects at USGS and CDMG strong motion stations in southern California and found that the small foundations and lightweight shelters used at most stations limited significant soil-structure interaction effects to frequencies on the order of 20-40 Hz. However, as pointed out by Crouse (2009), the soil softening that accompanies pore pressure generation in liquefiable soils will reduce the frequency range of soil-structure interaction effects by the same factor by which the soil stiffness is reduced. As a result, the motion recorded on the surface of a liquefied site may include soil-structure interaction effects following initiation of liquefaction.

Sloping Ground Effects. Some sites have sloping ground surfaces or are near enough to river banks or other free slope surfaces that non-zero shear stresses may exist on horizontal planes prior to earthquake shaking. Such shear stresses impose a static bias on the transient shear stresses induced by earthquake shaking and can cause asymmetric response strains accumulating preferentially in one direction and different stiffnesses in the upslope and downslope directions. Some one-dimensional site response analyses allow initial shear stresses to be approximated by "tilting" the soil profile by some small angle, but most do not.

Discussion. The preceding section has described a number of factors that can affect ground motions recorded by instruments on (or within) liquefiable soil deposits. These factors can exist at some sites and not others, and can be significant for some ground motions and not others. While some can be mitigated by, for example, more detailed subsurface investigation or instrumentation, others cannot. From the standpoint of the analyst seeking to validate a particular numerical code, it is perhaps most important to recognize that the recorded motion is likely to have been affected, to some degree, by factors that the numerical code was never intended to represent; as a result, a perfect match to the recorded motions should not be expected.

Example

One of the issues that distinguish nonlinear, effective stress site response analyses is the manner in which the contractive-dilative behavior of the soil is modeled. To examine the significance of this effect, the response of the Wildlife profile to the NS component of the 1987 Superstition Hills earthquake was analyzed using a code that ignores phase transformation behavior and one that models it explicitly. D-MOD2000 (Geomotions, 2007) was used for the former and WAVE (Horne, 1996) for the latter.

Both D-MOD2000 and WAVE are one-dimensional nonlinear effective stress site response analysis programs. The stress-strain behavior for the liquefiable sands in D-MOD2000 is based on the model proposed by Matasovic and Vucetic (1993), and incorporates softening due to the generation of excess pore pressure. The excess pore pressure is based on the Dobry et al. (1985) model as modified by Vucetic and Dobry (1988). The models used in D-MOD2000 do not account for phase transformation behavior. WAVE uses a relatively simple constitutive model for liquefiable sand (Kramer and Arduino, 1999) with a non-associative flow rule that allows representation of phase transformation behavior.

The NS component of the Superstition Hills event at the Wildlife site was analyzed using both D-MOD2000 and WAVE. The profile consists of four different soil types. To make the analyses as consistent as possible, the shear wave velocities and densities were assigned the same values and the hardening law in WAVE was adjusted to provide similar rates of softening to that used in D-MOD2000. The D-MOD2000 pore pressure parameters were those listed in Geomotions (2007) for the Wildlife silty sand. Pore pressure response in WAVE was controlled by the corrected SPT resistance of the silty sand layer, which was taken to be 13.95.

Figure 13 shows the recorded and predicted ground surface acceleration time histories. The D-MOD2000 time history predicts the recorded motion very well up to about 11 sec when it predicted very high pore pressures near the bottom of the liquefiable layer. Following the initiation of liquefaction, D-MOD2000 softened the lower portion of the silty sand layer to the point at which its shear strength did not allow significant acceleration levels to reach the ground surface; the D-MOD2000 post-liquefaction time history shows very low accelerations at very long periods. The WAVE time history matches the recorded time history reasonably well (but not quite as well as D-MOD2000) in the first 11 sec but did not predict very high pore pressures until 13-14 sec. WAVE then successfully models the transition to softer behavior and captures the major dilation-induced pulses that occur after the initiation of liquefaction. Both D-MOD2000 and WAVE predicted rates of pore pressure generation that were much faster than those recorded in the field. Figure 14 shows the recorded and predicted response spectra. The WAVE spectrum matches the recorded spectrum well at $T > 0.7$ sec, but falls below the recorded spectrum from about $0.05 - 0.7$ sec. The very low period portion of the WAVE spectrum is controlled by a dilation pulse and is somewhat higher than the recorded spectrum. The D-MOD2000 spectrum, on the other hand, falls below the recorded spectrum over a broad range of periods.
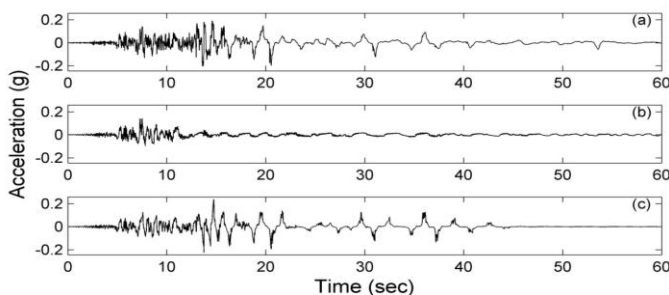

Fig. 13. NS ground surface accelerations for Superstition Hills at Wildlife Liquefaction Array: (a) recorded, (b) D-MOD2000 predicted, (c) WAVE predicted.
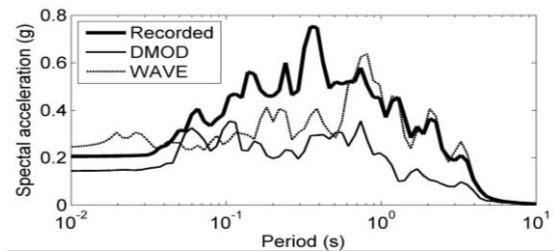

Fig. 14. NS response spectra for Superstition Hills at Wildlife Liquefaction Array.

EFFECTS OF LIQUEFACTION ON GROUND MOTIONS

Given that ground motions are sensitive to pore pressure generation and liquefaction, it is natural to consider the general nature of the effects of pore pressure generation on earthquake ground motions. Hartvigsen (2007) performed a series of parametric analyses using a nonlinear, site response program both with pore pressure generation (effective stress analysis) and without (total stress analysis). Nine 20-m-thick soil profiles with liquefiable layers representing all combinations of three thicknesses and three densities were developed, all with groundwater tables at 2 m depth. The profiles consisted of a layer of very dense gravel overlain by 4, 9, or 14 m of looser sands, thereby producing liquefiable layers of 2 m, 7 m, and 12 m thickness. The looser sands had $(N_1)_{60}$ values of 8, 16, and 24 blows/ft. All nine profiles were subjected to 139 input motions evenly distributed over 14 magnitude-distance bins.

Ground surface response spectra were computed for each input motion and each soil profile, once using total stress nonlinear analysis and once using effective stress nonlinear analysis. All analyses were performed using the same program so that the differences between the spectra were solely due to the effects of pore pressure generation. The effects of pore pressure on response were characterized by a response spectral ratio,

$$RSR(T) = S_a^{eff}(T) / S_a^{tot}(T) \qquad (1)$$

The response spectrum from the effective stress analysis was generally observed to fall below that of the total stress spectrum at low periods and to exceed it at intermediate periods. At long periods, the spectra were very close to each other. Analyses performed with input motions scaled to very low values ($PGA = 0.01$g) confirmed that the ground surface motions computed using both total and effective stress analyses were virtually identical, leading to the anticipated result that $RSR(T) \rightarrow 1.0$ as the level of earthquake shaking goes to zero (and as the factor of safety against liquefaction, $FS_L \rightarrow \infty$.

To characterize the "strength" of shaking with respect to liquefaction potential, Hartvigsen (2007) defined a loading parameter for a given element of soils as

$$L = \frac{a_{max}/MSF}{(a_{max}/MSF)_L} = \frac{CSR}{0.65 r_d} \frac{\sigma'_{vo}}{\sigma_{vo}} \Big/ \frac{CSR_L}{0.65 r_d} \frac{\sigma'_{vo}}{\sigma_{vo}} = \frac{CSR}{CRR} = \frac{1}{FS_L} \qquad (2)$$

The values of CRR were obtained by the procedure of Youd et al. (2001) with a_{max} taken as the peak ground surface acceleration computed in each total stress analysis. Dividing the results into a series of loading parameter bins showed consistent trends in the variation of $RSR(T)$ with both period and loading parameter. Figure 15(a) shows some variation in RSR(T) with period, but the values are relatively close to 1.0 since the loading parameter range of 0.4-0.6 implies high factors of safety against liquefaction on the order of 1.7-2.5. For loading parameters of 1.0-1.2 (i.e., factors of safety of 0.8-1.0), a significant reduction in spectral acceleration is observed (Fig. 15(b)) at periods below about 1 sec with an increase in spectral acceleration at periods above 1 sec. Figure 15(c) shows the same trend continuing at higher loading levels (lower factors of safety). It should be noted, however, that there is considerable scatter in the $RSR(T)$ values; further, the relatively jagged shapes of $RSR(T)$ plots for individual motions means that correlation in $RSR(T)$ residuals at different periods is low.
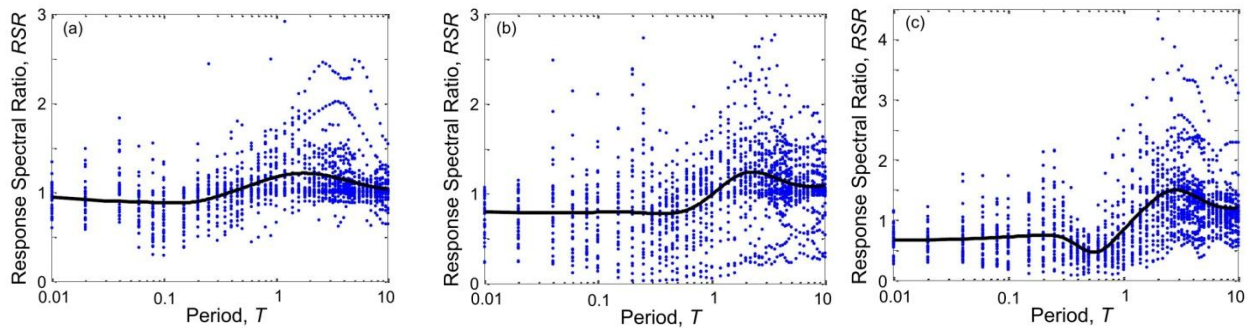

Fig. 15. Variation of response spectral ratio with period for: (a) 0.4 <L< 0.6, (b) 1.0 <L< 1.2, and (c) 1.8 <L< 2.0.

Hartvigsen (2007) combined the data from all of the analyses, found a functional form consistent with the behavior suggested by the loading bin plots (Fig. 15), and performed regression analyses to determine the coefficients of the function. Figure 16 shows the variation of RSR with both loading parameter and period. While the overall trend in response spectral ratio is well represented by the curved surface shown in Fig. 16, the relatively low correlation of the residuals indicates that the function is unlikely to capture the detailed effects of pore pressure generation on individual response spectra.

SUMMARY

Design and retrofitting of structures and facilities underlain by liquefiable soils requires the ability to predict the response of liquefiable soil profiles. Despite the high levels of damage caused by liquefaction in previous earthquakes, relatively few ground
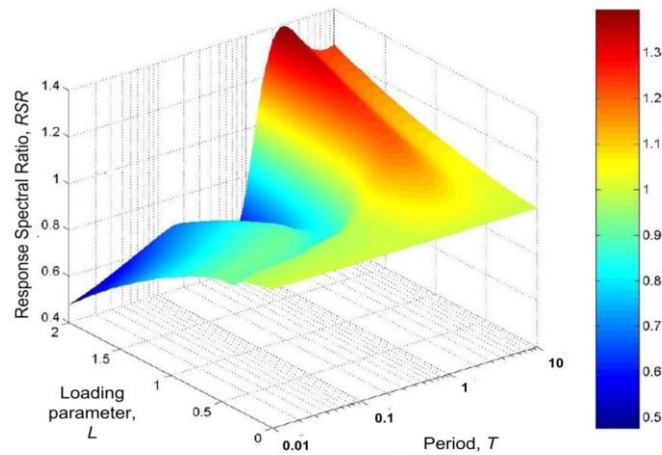
Fig. 16. Variation of mean response spectral ratio with period and loading parameter.

motions affected by liquefaction have been recorded, although the numbers appear to have increased within the past year. Liquefaction is known to cause dramatic and complicated changes in the stiffness of a soil profile, which cause its tendency to transmit waves of different frequencies to change with time. The generation of excess pore pressure in liquefiable soils tends to reduce the amplitude of high-frequency ground motion components and to increase the amplitude of longer-period components. Actual recordings, however, show complicated behavior in which high-frequency dilation pulses can occur and produce high accelerations even after liquefaction has been triggered. A number of constitutive models are able to represent the phase transformation behavior that leads this unique behavior. These models appear to more accurately represent the behavior of liquefiable soil profiles and to predict ground surface motions that are more consistent with available recordings.

REFERENCES

Boulanger, R. W., and Seed, R. B. [1995]."Liquefaction of sand under bi-directional monotonic and cyclic loading."*J. Geot. Eng.*, ASCE, 121[12]: 870-878.

Bonilla, L.F., Archuleta, R.J., and Lavallee, D. [2005]. "Hysteretic and dilatant behavior of cohesionless soils and their effects on nonlinear site response: Field data observations and Modeling," *Bull. Seism. Soc. Am.*, 95(6),2373-2395.

Crouse, C.B. [2009]. "Site-response analysis for liquefaction," Presentation at COSMOS 2009 Annual Meeting, (http://www.cosmos-eq.org/events/TS2009/presentations/2009_Crouse.pdf)

Crouse, C.B. and Hushmand, B. [1989]. "Soil-structure interaction at CDMG and USGS accelerograph stations," *Bull. Seis. Soc. Am.*, 79[1], 1-14.

Dobry, R., Pierce, W.G., Dyvik, R., Thomas, G.E., and Ladd, R.S. [1985]. "Pore pressure model for cyclic straining of sand." Research Report, Civil Engineering Department, Rensselaer Polytechnic Institute, Troy, NY, 56 p.

Earth Technology Corporation [1991]. "Accuracy of the porewaterpressures recoded at Wildlife site during magnitude 6.6 ImperialValley earthquake of 24 November 1987," Unpublished Report to U.S. Geological Survey, Reston, Virginia, 62 pp.

Geomotions. [2007]. "D-MOD2000 – A Computer Program for Seismic Response Analysis of Horizontally Layered Soil Deposits, Earthfill Dams and Solid Waste Landfills." Geomotions, LLC, Lacey, Washington.

Hartvigsen, A.J. [2007]. "Influence of pore pressures in liquefiable soils on elastic response spectra," *Master's thesis*, Univ. Washington, 150 pp.

Horne, J.C. [1996]. "Effects of liquefaction-induced lateral spreading on pie foundations." Ph.D. Dissertation, Univ. of Washington.

Hushmand, B., R. F. Scott, and C. B. Crouse [1991] "In-situ calibration of USGS piezometer installations," in *Recent Advances in Instrumentation, Data Acquisition, and Testing in Soil Dynamics*, S. K. Bhatia and G. W. Blaney [Eds], ASCE Spec. Pub. 29, 49–61.

Hushmand, B., R. F. Scott, and C. B. Crouse [1992]. "In-place calibration of USGS pore pressure transducers at Wildlife Liquefaction Site, California, USA," in *Proc. 10th Earthquake Engineering World Conference*, Balkema, Rotterdam, The Netherlands, 1263–1268.

Iai, S., Y. Matsunaga, and T. Kameoka [1990]. "Strain space plasticitymodel for cyclic mobility," Report of the Port and Harbor Research Institute, 29, 27–56.

Idriss, I.M. and Boulanger, R.W. [2008]. *Soil liquefaction during earthquakes*, Monograph MNO-12, Earthq. Eng. Res. Inst., 235 pp.

Ishihara, K. (1985). "Stability of natural deposits during earthquakes," *Proceedings*, Eleventh Int. Conf.Soil Mech. Found. Eng., 1, 321-376.

Kramer, S.L. and Arduino, P. [1999]. "Constitutive modeling of cyclic mobility and implications for site response," Proceedings, Earthq.Geotech. Eng., P. Seco e Pinto, ed., Balkema, 3, 1029-1034.

Kutter, B.L., and Wilson, D.W. [1999] "De-liquefaction shock waves," 7th U.S.- Japan Workshop on Earthquake Resistant Design of Lifeline Facilities and Countermeasures Against Liquefaction", Seattle Washington, *Technical Report MCEER-99-0019,* O'Rourke, Bardet, and Hamada, eds., 295-310.

Manzari M.T. andDafalias Y. F. [1997], "A critical state two-surface plasticity model for sands," *Geotechnique*, 47[2], 255-272.

Martin, G.R., Finn, W.D.L., and Seed, H.B. [1975]. "Fundamentals of liquefaction under cyclic loading," *J.Geot. Eng. Div.,* ASCE, 101[GT5], 423-438.

Masing, G. [1926]. "Eigenspannungen und verfestigungbeim messing [self stretching and hardening for brass]."*Proc.*, 2nd Int. Congress for Applied Mechanics, Zurich, Switzerland, 332–335.

Matasovic, N. and Vucetic, M. [1993]."Cyclic characterization of liquefiable sands." *ASCE J. Geotech. Eng.,* 119(11), 1805-1822.

Mayfield, R.T. [2007]. "The return period of soil liquefaction," *Ph.D. Dissertation*, Dept. of Civil and Env. Eng., Univ. of Washington, 272 pp.

Muravskii, G. [2004]. "On description of hysteretic behavior of materials," *Int. J. Solids and Sturct.*, 42, 2625-2644.

Nakamura, Y. [1989]. "A method for dynamic characteristics estimation of subsurface using microtremor on the ground surface," *Quart. Rep.*, Rail. Tech. Res. Inst., 30(1), 25-33.

Phillips, C. and Hashash, Y.M.A. [2009]. "Damping formulation for nonlinear 1D site response analyses," *Soil Dyn. Earthq. Eng.*, 29, 1143-1158.

Pyke, R.M. [1973]. "Settlement and liquefaction of sands under multi-directional loading," *Ph.D. dissertation*, Univ. Calif., Berkeley.

Pyke, R.M. [1979]. "Nonlinear soil models for irregular cyclic loadings," *Jour. Geot. Eng. Div.*, ASCE, 105(GT6), 715-726.

Scott, R. F., and B. Hushmand [1995].Discussion of "Piezometer at Wildlifeliquefaction site," by T. L. Youd and T. L. Holzer, *J. Geotech.Eng. ASCE* 121, 912–919.

Vucetic, M. and Dobry, R. [1988] "Cyclic triaxial strain-controlled testing of liquefiable sands." Advanced Triaxial Testing of Soil and Rock, ASTM STP 977, American Society for Testing and Materials, Philadelphia, pp. 475-485.

Yang, Z., Elgamal, A., and Parra, E. 2003."A computational model for liquefaction and associated shear deformation,"*J. Geot. And Geoenv. Eng.*, ASCE 129[12]: 1119-1127.

Youd, T. L., and B. L. Carter [2005]. "Influence of soil softening and liquefaction on spectral acceleration," *J. Geotech. Geoenviron. Eng. ASCE* 131, 811–825.

Youd, T. L., and T. L. Holzer [1994]. "Piezometer performance at Wildlife liquefaction site," California, *J. Geot. Eng. ASCE* 120, 975–995.

Zeghal, M., and A. W. Elgamal [1994]."Analysis of site liquefaction using earthquake records,"*J. Geotech.Eng.* 120, no. 6, 996–1017.